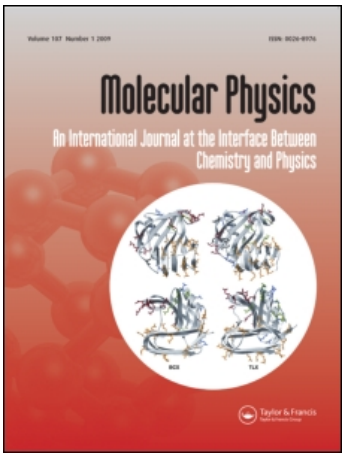

Molecular Physics
Publication details, including instructions for authors and subscription information:
http://www.informaworld.com/smpp/title~content=t713395160

Simulated quantum computation of global minima

Jing Zhu [a]; Zhen Huang [a]; Sabre Kais [a]
[a] Department of Chemistry and Birck Nanotechnology Center, Purdue University, West Lafayette, IN 47907, USA

First Published:June2009

To cite this Article Zhu, Jing, Huang, Zhen and Kais, Sabre(2009)'Simulated quantum computation of global minima',Molecular Physics,107:19,2015 — 2023
To link to this Article: DOI: 10.1080/00268970903117126
URL: http://dx.doi.org/10.1080/00268970903117126

Molecular Physics
Vol. 107, No. 19, 10 October 2009, 2015–2023

Taylor & Francis
Taylor & Francis Group

RESEARCH ARTICLE

Simulated quantum computation of global minima

Jing Zhu, Zhen Huang and Sabre Kais*

Department of Chemistry and Birck Nanotechnology Center, Purdue University, West Lafayette, IN 47907, USA

(*Received 27 February 2009; final version received 11 June 2009*)

Finding the optimal solution to a complex optimisation problem is of great importance in practically all fields of science, technology, technical design and econometrics. We demonstrate that a modified Grover's quantum algorithm can be applied to real problems of finding a global minimum using modest numbers of quantum bits. Calculations of the global minimum of simple test functions and Lennard-Jones clusters have been carried out on a quantum computer simulator using a modified Grover's algorithm. The number of function evaluations N reduced from $O(N)$ in classical simulation to $O(N^{1/2})$ in quantum simulation. We also show how the Grover's quantum algorithm can be combined with the classical Pivot method for global optimisation to treat larger systems.

Keywords: quantum computation; Grover's quantum algorithm; Pivot method; clusters; global optimisation

Rational drug design, molecular modelling, quantum mechanical calculations and mathematical biological calculations are but a few examples of fields that rely heavily upon the location of a global minimum in a multiple-minima problem [1–6]. Several global optimisation methods have been developed over the past decades. However, the large computational cost of finding the global minimum for a large number of variables limited the applications of such algorithms [7–10]. Quantum algorithms on the other hand are known to speed up the computation compared to classical ones [11–14]. For example, the calculation time for the energy of atoms and molecules scales exponentially with system size on a classical computer but polynomially using quantum algorithms [15,16].

Quantum computation is generally regarded as being more powerful than classical computation. The evidence for this viewpoint begins with Feynman's pioneering observation [17] that the simulation of a general quantum evolution on a classical computer appears to require an exponential overhead in computational resources compared to the physical resources needed for a direct physical implementation of the quantum process itself. Subsequent work by Deutsch [18], Bernstein and Vazirani [19], Simon [20], Grover [21], Shor [22,23] and others showed how quantum evolution can be harnessed to carry out some useful computational tasks more rapidly than by any known classical means. For some computational tasks (such as factoring) quantum physics appears to provide an exponential benefit, but for other tasks (such as NP complete problems [24]) the quantum benefits appear to be inherently more restricted, giving at most a polynomial speedup [25–30].

Grover's quantum algorithm can find an object in a unsorted database containing N objects in $O(N^{1/2})$ quantum mechanical steps instead of $O(N)$ steps [31,32]. The steps of Grover's algorithm can be shown as following: firstly, the Walsh–Hadamard transformation was performed and the system was initialised to the superposition. Before going any further, let's introduce some fundamental information of quantum simulation [33]. Quantum computation and quantum information are built upon the concept the *quantum bit*, or *qubit* briefly. It is quite similar to a bit in classical computation. Two possible states for a qubit are the states $|0\rangle$ and $|1\rangle$, which is similar to state 0 and 1 for a classical bit. The difference between bits and qubits is that a qubit can be in a state other than $|0\rangle$ or $|1\rangle$. It is also possible to form a linear combination of states, called *superpositions*:

$$|\psi\rangle = \alpha|0\rangle + \beta|1\rangle, \tag{1}$$

*Corresponding author. Email: kais@purdue.edu

ISSN 0026–8976 print/ISSN 1362–3028 online

DOI: 10.1080/00268970903117126
http://www.informaworld.com

where α and β are complex numbers and $|\alpha|^2 + |\beta|^2 = 1$. Furthermore, one famous qubit gate is the *Hadamard gate*, and it is defined as:

$$H \equiv \frac{1}{2^{1/2}} \begin{pmatrix} 1 & 1 \\ 1 & -1 \end{pmatrix}. \tag{2}$$

This gate is also described as being like a 'square-root of not' gate, in that it turns a $|0\rangle$ into $(|0\rangle + |1\rangle)/2^{1/2}$ (first column of H), 'halfway' between $|0\rangle$ and $|1\rangle$; and turns $|1\rangle$ into $(|0\rangle - |1\rangle)/2^{1/2}$ (second column of H), which is also 'halfway' between $|0\rangle$ and $|1\rangle$. In our simulation, we performed the Hadamard transform on n qubits initially for all $|0\rangle$ states and obtained an equal superposition of all computational basis states. Mathematically it could be expressed by the following formula:

$$|s\rangle = \bigotimes_{i=1}^{n} H|0\rangle, \tag{3}$$

where $|s\rangle$ means the initial superposition and n means the number of qubits. Secondly, we generated two different operators called P_s and P_t. Their mathematical formations are $P_t = I - 2|t\rangle\langle t|$ and $P_s = 2|s\rangle\langle s| - I$, where $|s\rangle$ is the initial superposition and $|t\rangle$ corresponds to the entry matching the search criterion. In practice, there are no direct universal quantum algorithms currently to obtain $|t\rangle$ besides the 'black box function' or the 'oracle' [33,34]. In order to get $|t\rangle$ here, we first did a classical comparison based on a search criterion and then translated the result into the quantum state. The detailed procedure is provided in Appendix 1. The physical meaning of P_t is performing the selective phase inversion, and that of P_s is performing the inversion about an average operation, which increases the amplitude of the state which was inverted in the previous step. Finally, we applied the Grover operator, $G = P_s P_t$, $O(N^{1/2})$ times to the superposition state. After performing the measurement to the obtained vector, the one with the max probability is the marked state [31,32]. Grovers' search algorithm has been implemented by using nuclear magnetic resonance (NMR) techniques for a system with four states [35] and more recently using quantum optical methods [36]. An efficient quantum algorithm for global optimisation based on such Grover's search procedure can find applications in a wide range of fields [37].

In this paper, we will demonstrate that a modified Grover's quantum algorithm can be applied to real problems of finding a global minimum using modest numbers of quantum bits. We will simulate the revised quantum search algorithm using a classical computer. The limitation of a computer resource such as the memory and speed of a CPU will prohibit a large scale quantum computer algorithm simulation on a classical computer. Thus, first we implement the algorithm for simple test functions and small size Lennard-Jones clusters. The quantum search circuit is shown in Figure 1. In this figure, we divided the register into three groups, where the Hadamard gates are operated on the initialised registers, then we applied the Grover iteration to rotate the superposition states into target states. The measurement result after the iteration is used to update the threshold value in the Grover iteration steps. The Grover oracle is replaced by the adapted threshold to search all the states for which $f(x_1, x_2, \ldots) \le M_{n-1}$, where M_{n-1} gives the minimum measurement value. The subscript n denotes the steps of measurements and M_n denotes the value of the nth measurement. The iteration number during each search will be preselected. After each iteration, the result will be measured and compared with the other measured results to set up a new threshold value.

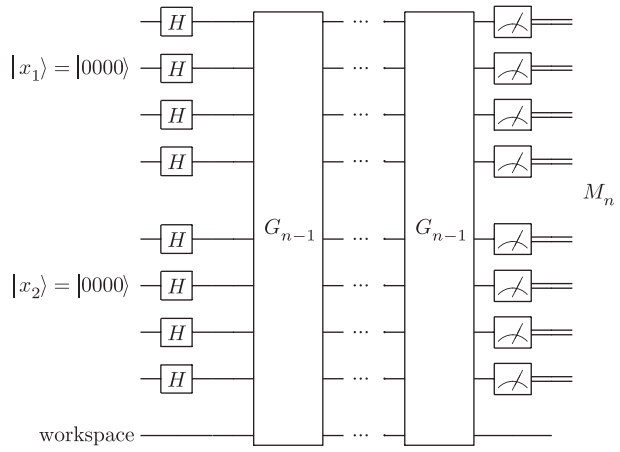

Figure 1. Quantum circuit for searching the global minimum. The G_{n-1} is the oracle to rotate the vector toward the state with $f(x_1, x_2, \ldots) \le M_{n-1}$, where M_{n-1} is the minimum of all measurement results. The registers will be initialised to $|x_1\rangle = |0000\rangle$ and $|x_2\rangle = |0000\rangle$ for variable x_1 and x_2. After using the Hadamard gates to convert the initial state into the superposition state, the adapted Grover operators will be applied to rotate the superposition state to the specific state. The threshold value of Grover's operator will be updated based on the measurement result after a certain number of rotations.

We first applied the adapted quantum search algorithm to test a simple analytical function used in global optimisation: the Goldstein–Price function (GP) which is given by [10]

$$\begin{aligned} f(x_1, x_2) = \big[1 + (x_1 + x_2 + 1)^2 (19 - 14x_1 + 3x_1^2 - 14x_2 \\ + 6x_1x_2 + 3x_2^2)\big]\big[30 + (2x_1 - 3x_2)^2 (18 - 32x_1 \\ + 12x_1^2 + 48x_2 - 36x_1x_2 + 27x_2^2)\big], \end{aligned} \tag{4}$$

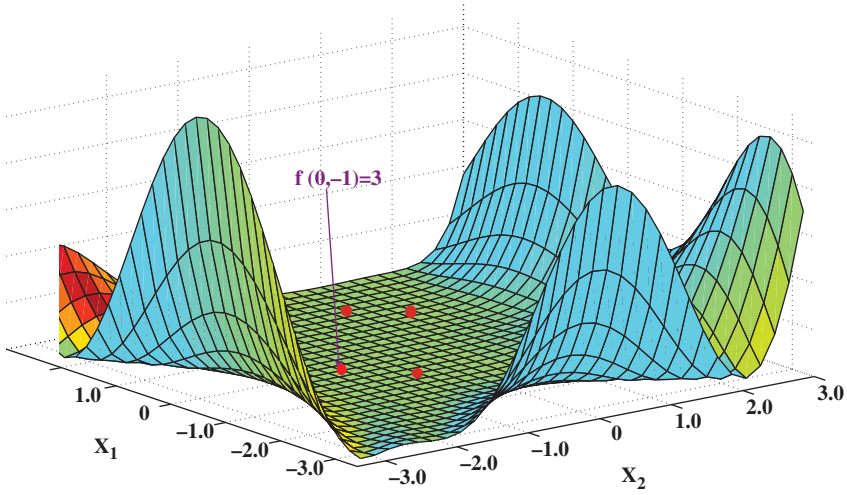

Figure 2. The potential surface near the global minimum of the GP function (see the text). It is difficult to tell the four minima points visually on a scale of zero to five million, so they are marked by brown circles. $f(0,-1)=3$ is the global minimum which is indicated by the arrow.

where $-2 \le x_i \le 2$. The GP function is an excellent test function for any global optimisation method, which has four local minima in the whole region. One global minima is located at $(0, -1)$ with the function equal to 3, the other three local minima are $f(-0.6, -0.4) = 30$, $f(1.8, 0.2) = 84$ and $f(1.2, 0.8) = 840$. The potential surface near the global minimum is shown in Figure 2. It is kind of difficult to visual minima on a scale of 0 to five million. We added four brown circles to mark all local minima positions, furthermore, the global minima $f(x_1, x_2) = 3$ is shown by the arrow in Figure 2. We used 10 qubits as the registers (as an example, see Appendix 1 for detailed calculations using two qubits). The registers will be divided into two groups to present the variable x_1 and x_2. The searching range is $x_{1,2} \in [-3.2, 3.0]$, which covers all local and global minima. After applying the Hadamard gate, the registers group will be initialised into the superposition state, each will be used to cover 2^5 discrete points in the searching range, namely, each basis function will be mapped to the number within the searching domain. Then, the measurement will be performed to obtain the first threshold value after the selected number of Grover iterations was applied. The number of iterations before each measurement is important to reduce the total iteration number. We chose the sequence: 0, 0, 0, 1, 1, 0, 1, 1, 2, 1, 2, 3, 1, 4, 5, 1, 6, 2, 7, 9, 11, 13, 16, 5, . . . , as the iteration number before each measurement, i.e. for step 1 we measure the state without any Grover iteration, for step 4, we measure the state after one Grover iteration. This sequence was proposed in [38] to reduce the Grover iteration numbers for the adopted Grover search method. During each iteration, the state function will be rotated towards the threshold value, which is always the best measurement result at previous steps. The new obtained value will be compared with the old threshold value. The threshold value will be reset to the new value if the old threshold value is larger than the new measurement result, otherwise it is unchanged. The iteration will continue until convergence is reached. The quantum search yields the same result (high probability) as the classic method with 16 steps. In Figure 3, we show the probability distribution of the state function before the iteration steps. The top left panel is the initial state, where the state function is the superposition for every possible state, and the measurement result yields 379,605.8306 after step 1 without any Grover iteration. In Figure 3, panel (b) is the state function after a total of two Grover iterations at step 5, where the measurement result yields 4038.3764. As we can see the probabilities for smaller function values become larger, meanwhile the eigenfunction corresponding to larger function values starts decreasing. In panel (c), the area of high probability reduced a lot compared with panel (b). It means that the search keeps converging at step 10. At step 16 with a total of 22 Grover iterations, we reach the global minimum value 3 at $x_1 = 0$ and $x_2 = -1$ as shown in panel (d) of Figure 3.

Let us further illustrate this approach by considering a real and practical optimisation problem: finding the global minimum of Lennard-Jones clusters, clusters of atoms or molecules that interact with each other through the Lennard-Jones potential. The Lennard-Jones potential (referred to as the L-J potential or 6–12 potential) is a simple mathematical model that

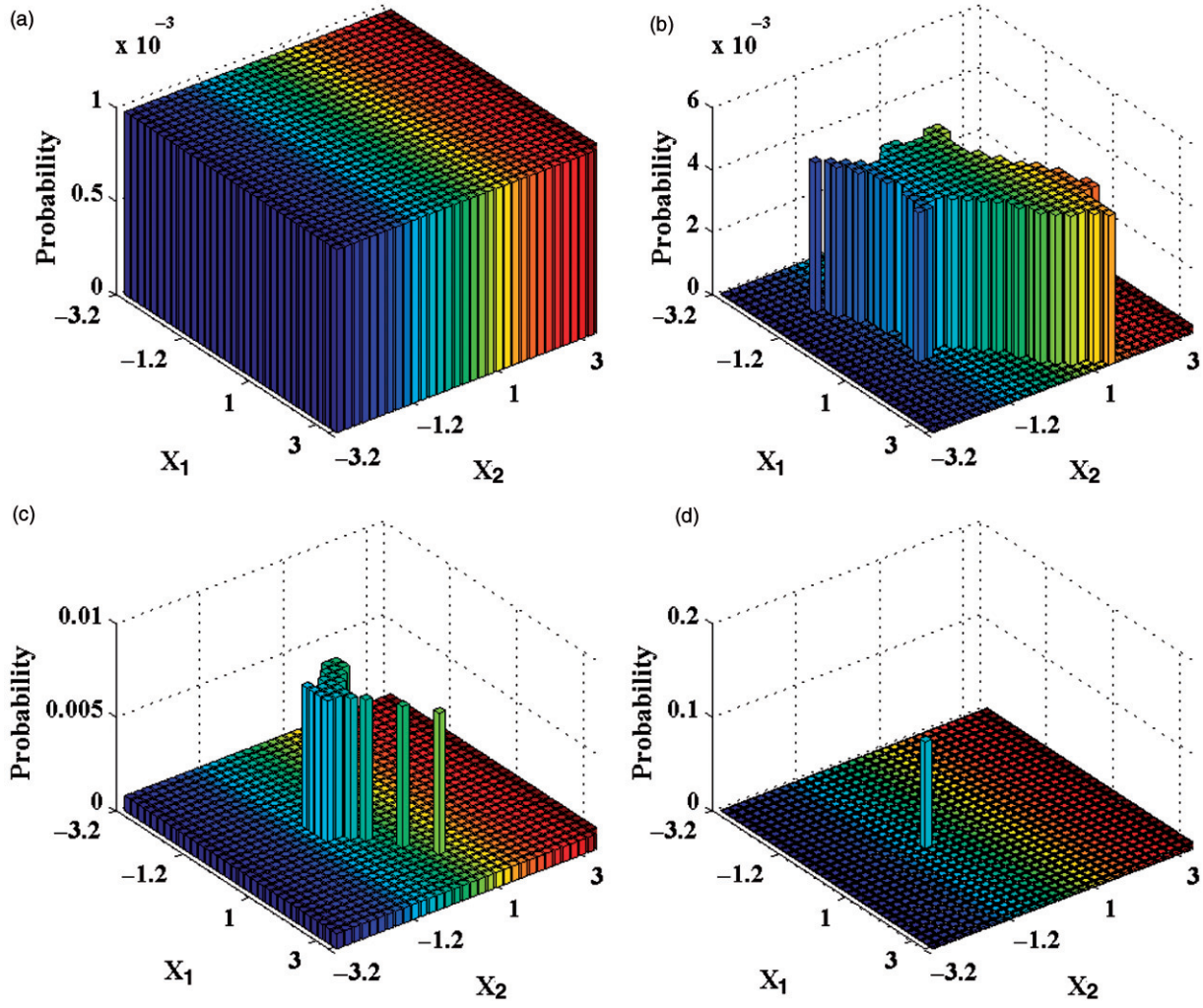

Figure 3. Probability distribution of the state function before the measurement for the GP function. Panel (a) is the initial state corresponding to the superposition of all possible states, panels (b), (c) and (d) are the distributions of step 5, 10 and 16 respectively.

describes the long range attractive van der Waals force and the short range Pauli repulsion force. The L-J potential is of the form:

$$V_{\mathrm{LJ}}(r) = \epsilon\left[\left(\frac{2^{1/6}\sigma}{r}\right)^{12} - \left(\frac{2^{1/6}\sigma}{r}\right)^{6}\right], \qquad (5)$$

where ϵ and $2^{1/6}\sigma$ are the pair equilibrium well depth and separation, respectively. r is the relative distance between two particles. We will employ reduced units in our simulation and define $\epsilon = 2^{1/6}\sigma = 1$. The L-J potential is a relatively good approximation and due to its simplicity often used to describe the properties of gases, and to model dispersion and overlap interactions in molecular models. It is particularly accurate for noble gas atoms and is a good approximation at long and short distances for neutral atoms, molecules and clusters. Lennard-Jones clusters are excellent for testing the efficiency of global optimisation algorithms [39]. Homogeneous Lennard-Jones clusters have well-established minima and regular minimum-energy structures for very large clusters [40]. However, the number of local minima apparently grows rapidly and finding the global minimum in Lennard-Jones clusters is an NP-hard problem [41]. Several global optimisation methods have been applied to the energy function of Lennard-Jones clusters. The total energy for a Lennard-Jones cluster of M particles is: $E_M = \sum_{i=1}^{M-1} \times \sum_{j=i+1}^{M} V_{\mathrm{LJ}}(r_{ij})$, where r_{ij} is the distance between the ith and the jth particles and $V_{\mathrm{LJ}}(r)$ is the Lennard-Jones two-body potential. We start simulating the process of searching the global minimum for $M = 3$ particles. A total of nine register qubits ($N = 2^9 = 512$ mesh points) were separated into two groups for presenting

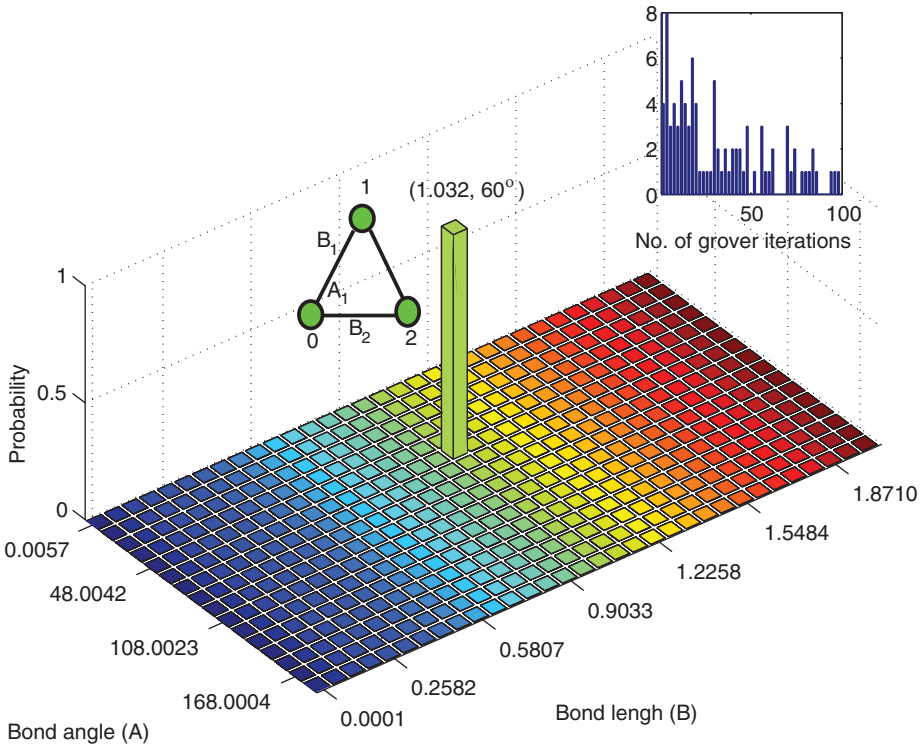

Figure 4. Final probability distribution of the state function for LJ ($N=3$). The global minimum located at $B_1=1.0323$, $B_2=1.0323$ and $A_1=1.0473$ rad $=60^\circ$. The top panel is the distribution of the total measure step before reaching the global minimum for 100 search results. The global minimum and corresponding structure are also shown in the figure.

three variable B_1, B_2, and A_1, where B_1 is the bond length between the atom 0 and 1, B_2 is the bond length between atom 0 and 2, and A_1 is the bond angle of atom 0, 1 and 0, 2 as shown in Figure 4. Five qubits will be used as the first register to cover the space $B_1=B_2$, and four qubits will be used as the second register for A_1. The searching range for $B_{1,2}\in[0.0001,2]$ and for $A_1\in[0.0001,\pi]$. The quantum search yields the minimum value -2.9094 at $B_1=1.0323$, $B_2=1.0323$ and $A_1=1.0473$ rad $=60^\circ$. Compared with the classical minimum potential, it is slightly higher. This is due to the fact that our mesh can not cover the exact minimum value. Unlike the search method for GP function, where the number of iterations is preselected based upon the proposed sequence, here we increase the number of iterations after every measurement to study the importance of the iteration sequence. The number of iterations increases as $1,2,3,4,\ldots$. In Figure 4, we show the search results and the total iteration steps. From the histogram of total number of iterations for 100 independent searches, we found that the average number of iterations is about 21. This indicates that the running time of the adapted search algorithm (a total of 231 iterations) is still the same as the Grover search algorithm $O(N^{1/2})$, which is about $10(2^9)^{1/2}$ in this example. The configuration corresponding to the minimum for the LJ cluster is also shown in Figure 4.

In order to expand the adapted quantum search algorithm to search the global minimum for larger number of variables and to overcome the limit of using a large number of qubits in the computation, we combined the classical pivot search method [9,10] with the quantum Grover's search algorithm. The basic scheme is as following: *Step (1)*: Generate N random probes, where N is equal to $2^{\text{number of qubits}}$, then shift it into superposition of the entire state space. *Step (2)*: Use the quantum Grover algorithm mentioned before to do the comparison. Select and keep about the smallest 15% of the original N random probes as pivot probes. *Step (3)*: Initialise the quantum computer with the state associated with these pivot probes, apply a series of controlled Hadamard gates to produce the superposition state with points near the selected probes. $x_{R,i}=x_{B,i}+\Delta x_i$, where Δx_i is a randomly generated vector according to a particular distribution such as a Gaussian distribution [9]. *Step (4)*: Redo *Step (2)* and keep going until the criteria of convergence is satisfied. Using this procedure, it is possible to cover the entire searching space by a small number of qubits. Moreover, this small number of qubits is sufficient to cover each subdomain to yield the desired resolution.

To illustrate this combined approach, we search the global minimum for the Shubert test function, which is given by [10]:

$$f(x_1, x_2) = \left[\sum_{i=1}^{i=5} i\cos[(i+1)x_1 + i]\right] \times \left[\sum_{i=1}^{i=5} i\cos[(i+1)x_2 + i]\right] \quad (6)$$

with $-10 \le x_{1,2} \le 10$, which has 760 local minima, 18 of which are global with $f(x_1, x_2) = -186.7309$. The surface potential of this function is shown in Figure 5. Ten qubits were used to do this simulation, each x was assigned five qubits. Following the same procedure mentioned above, we initially generated 2^{10} random points. Then 15% minimum of these points were picked up by quantum Grover algorithm as pivots. After that, we arranged the pivots based on the weight of the optimised function ($\exp(-f(x_1, x_2)/kT)$), where kT is just a fixed parameter and is equal to 50 in our simulation. We generated the other points according to the Gaussian distribution. We ran this simulation for 98 times, the researched minimum values are between -30.56 and -186.73. Over 80% of the points are located at -186.73, which is the exact global minimum for this function. It also covers all 18 global minima and the average iteration is 1300. The simulation results are shown in Figure 5, where the black dots are measurement results on the contour of the surface potential with red dots as global minima. It seems this method only converges to the global minima 80% of times. However, the advantage is that only 10 qubits are used, which means 2^5 pivot points for each x axis, with a total of 2^{10} mesh points. It is a very small mesh based on a current computer. If we can use 20 qubits (10 for each axis), the number of mesh points will be much larger. Under this situation, the convergence speed will be much faster.

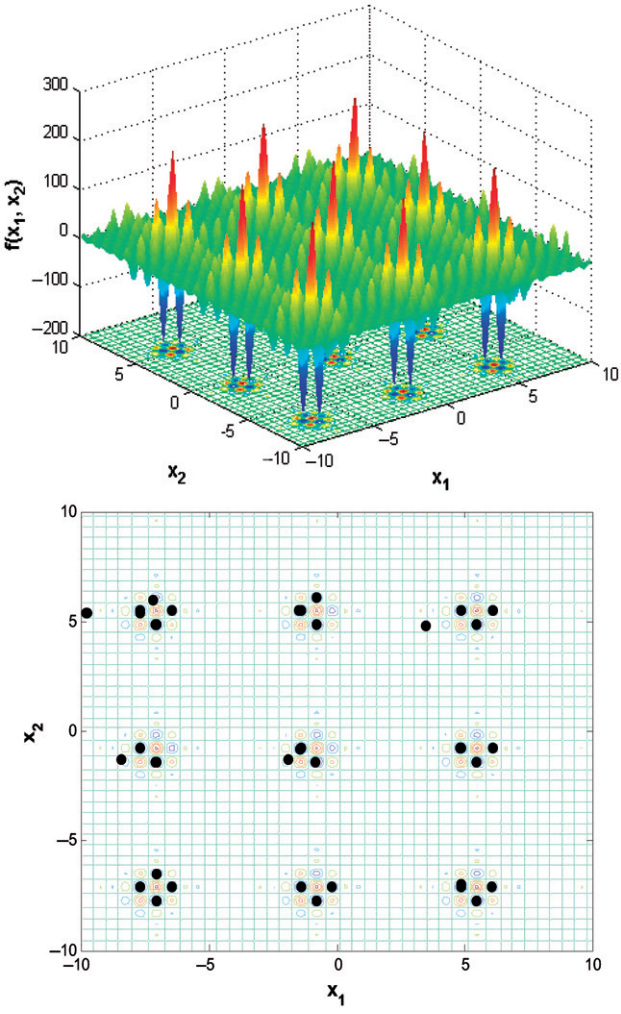

Figure 5. The surface potential of the Shubert function and the final quantum search results. The top panel is the surface potential for the Shubert function with the range $x_{1,2} \in (-10, 10)$. The bottom panel is the contour of the function with the quantum search results. The black dots present the measurement results for all search steps.

Furthermore, following the same steps, we also applied this combined method to search for the optimised structure for LJ clusters. We tried five atoms and got the exact same results as the classical method. The detailed procedure for the three-atom simulation is as following: we first set five qubits for $B_{1,2}$ and five qubits for A_1. The same previous range, which is $B_{1,2} \in [0.0001, 2]$ and for $A_1 \in [0.0001, \pi]$. We first generated 2^5 random $B_{1,2}$ and 2^5 random A_1 in the above range. Then we used the combined classical pivot method and Grover's search algorithm which was mentioned in the previous paragraph. After the search, we got the global minimum structure for the three-atom cluster (the same structure shown in Figure 4). The distance between each atom is 0.99889 and the total potential for this structure is -2.9999, which is almost the same as the classical result (-3.0). After that, based on the optimised structure of three atoms, we added another atom to form the four-atom cluster. We fixed the original three atoms and set the fourth one free. We used X, Y and Z to express the coordinates for the fourth atom and used 10 qubits in the simulation, the same number as in the previous simulations. We tried two different ways to perform the simulations: in the first method, we left the fourth atom totally free in the X, Y and Z directions and set four qubits for the X axis, three qubits for the Y axis and three qubits for the Z axis. In order to save simulation steps, the ranges for all coordinates are $X \in [-0.5, 0.5]$, $Y \in [0.01, 1.01]$ and $Z \in [0.01, 1.01]$. Then we followed the same steps as for three atoms, generated random points and started the

search. After a number of simulations, the result converged to −5.0, on average, which is not quite accurate (classical = −6.0). The second method is fixing X at 0.0 and arranging five qubits for Y and Z respectively. The ranges for Y and Z are the same, between 0.01 and 1.01. The rest of the procedure is the same as for three atoms. The simulation results giving the lowest potential for this cluster is −5.9926, which is quite close to the classical result (−6.0). The probability distribution for the whole procedure is shown in Figure 6, as well as the final structure. We stepped forward to apply this method to simulate the most optimised structure for a five-atom cluster. The simulation procedure is the same as for the four-atom cluster. We fixed the previous optimised structure and added the 5th free atom. We also used the above two methods, and results show that the second method gave more accurate results. We obtained the value −9.0952, which is close to the classical simulation value (−9.103852). Although we did not get the exact optimised structures with the current simulations, however with more qubits one should cover the exact results.

It is known that $N^{1/2}$ is the optimal running time for a quantum search algorithm. The combined search method does not reduce the total rotation steps, but does reduce the required number of qubits to do the simulation. Due to the limited available qubits in a classical computer, we can only set one atom free with all other atoms fixed. However, in a quantum computer, with enough qubits available, we can perform full optimisation for all atoms. For example, for larger LJ clusters, if we had larger qubits, we could incorporate the partial knowledge that we had by starting with the structure of the smaller $(M-k)$ clusters and adding k additional particles at random [9,42]. In a previous

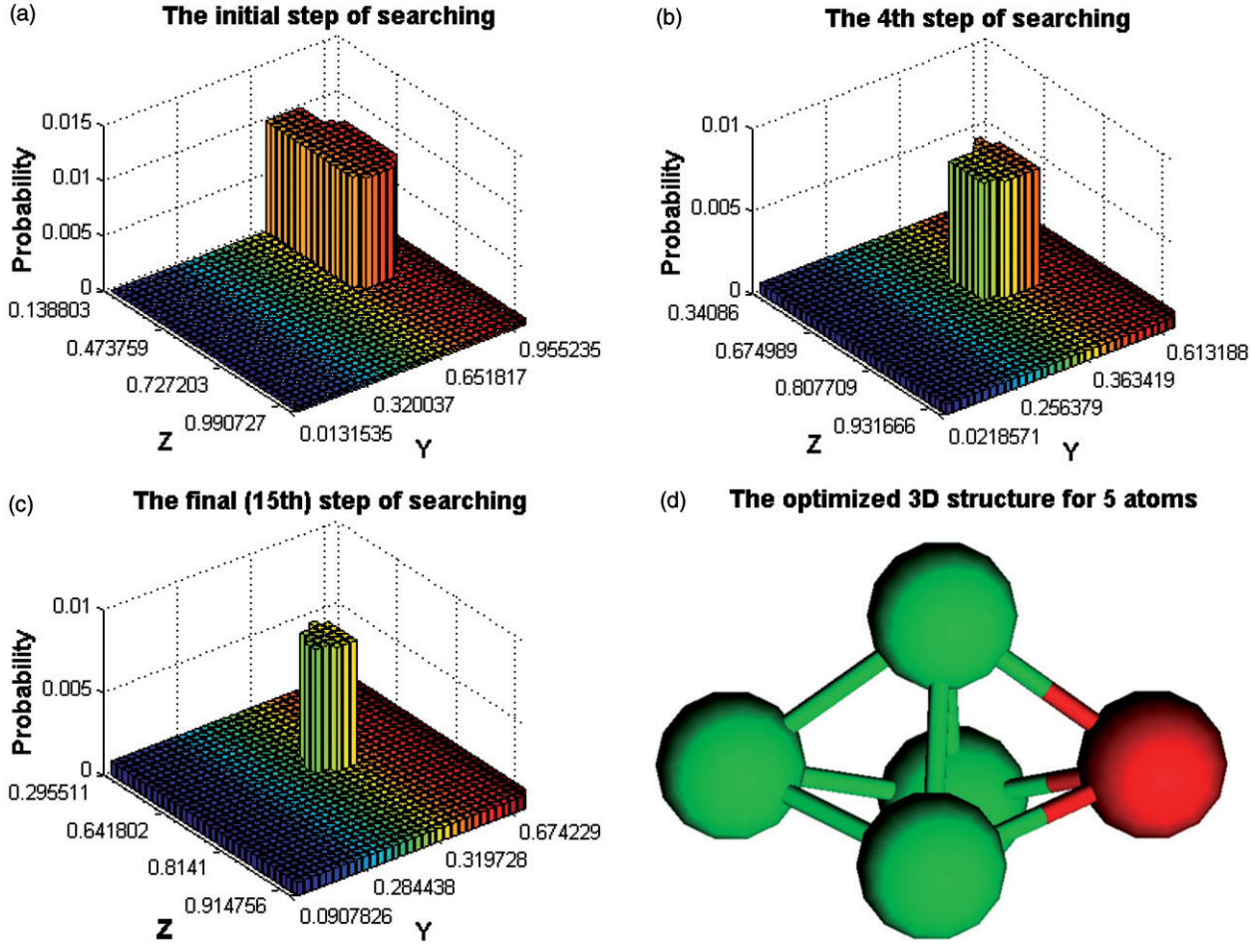

Figure 6. Probability distribution of the state function for LJ cluster ($N = 4$). Panels (a), (b) and (c) are the steps during the searching. The global minimum energy is −5.9926 and the coordinates for the fourth atom are (0.0, 0.28444, 0.81344). Although there are many bars, they are quite close to each other. Panel (d) is the optimised structure for a five-atom cluster with an energy of −9.0952. The green atoms are fixed atoms, while the red one is the free atom. The distances between the red and the green ones are 0.99, 0.99 and 1.00 separately.

work [9], using the pivot method we have shown that the computational cost (CPU time) scales as $M^{2.9}$ with the number of L-J particles to be minimised. With various practical improvements, one can reduce the scale to M^2. If we can assign a certain number of qubits for each particle, then the Grover algorithm will reduce the search steps to the order of $O(M)$ for this specific case. In any 'growing' problem, such as the minimum energy configuration of clusters, self-avoiding walks, protein folding, etc., this systematic approach to solving the structure of large clusters can be incorporated. One of the powerful features of this combined algorithm is that information such as this can be built into the initialisation of the probes.

We have used an adapted quantum search algorithm to search the global minima for test functions and LJ clusters. Our quantum computer simulations on the classical computer yield the same global minimum values as the classical search method with high probability. We also show how to combine the classical Pivot method with the adapted quantum search algorithm to search for the global minimum in larger domains. Recently, Jordan [43] proposed a fast quantum algorithm for estimating numerical gradients with one query. One can use this method to search the potential gradient with zero value. This will rotate the entire space towards the state function which corresponds to all minima. The measurement will yield one of the minima instead of any point in the search domain. Combining this with our search method will greatly reduce the number of rotations needed for finding the global minimum. With further improvements in the quantum search algorithms, we expect to see solutions of previously intractable global optimisation problems in many different fields.

In summary, the manuscript contains novel results and a proof-of-principle about the use of quantum computers for the simulation of a global minimum. First, the paper provides fundamental insight into the quantum simulation of global optimisation problems, and second we implemented some simple applications. We also demonstrated for the first time that a modified Grover's quantum algorithm can be applied to real problems of finding a global minimum using a modest number of qubits. If a quantum computer that would allow for these calculations to be carried out were available now, we believe that the development of algorithms for optimisation is of great importance in many practical fields and further motivates the construction of these devices.

Experimentally, the Grover's algorithm has been demonstrated by nuclear magnetic resonance (NMR) [44–48] and quantum optics [36] for a small number of qubits. Although it is easy to obtain the Grover's oracle by classic computers, it is very hard to realise this oracle in a quantum circuit. There are no efficient universal methods to design this oracle until now. Recently there have been a few attempts to solve this problem directly. Ju *et al*. [49] implemented Grover's oracle function by Boolean logic in a quantum circuit. However, they used N ($2^{number\ of\ qubits}$) Boolean logic to represent the oracle, which makes the circuit design inefficient. On the other hand, Xu *et al*. [50] successfully used the adiabatic search algorithm to realise Grover's algorithm without oracle by encoding the database to quantum format and forming the problem Hamiltonian form target value. Further research is still needed to overcome the Grover's oracle.

Acknowledgements

We thank Jonathan Baugh for useful discussions and the Army Research Office (ARO) for funding.

References

[1] S. Kirkpatrick, C.D. Gelatt Jr, and M.P. Vecchi, Science **220**, 671 (1983).
[2] J. Barhen, V. Protopopescu, and D. Reister, Science **276**, 1094 (1997).
[3] D. Cvijovis and J. Klinowski, Science **267**, 664 (1995).
[4] D.J. Wales and H.A. Scheraga, Science **285**, 1368 (1999).
[5] P. Nigra and S. Kais, Chem. Phys. Lett. **305**, 433 (1999).
[6] S. Kais and R.D. Levine, J. Phys. Chem. **91**, 5462 (1987).
[7] D.E. Goldberg, *Genetic Algorithms in Search, Optimization and Machine Learning* (Addison Wesley, Reading, MA, 1989).
[8] D.D. Frantz, D.L. Freeman, and J.D. Doll, J. Chem. Phys. **93**, 2769 (1990).
[9] P. Serra, A.F. Stanton, and S. Kais, Phys. Rev. E **55**, 1162 (1997).
[10] P. Serra, A.F. Stanton, S. Kais, and R.E. Bleil, J. Chem. Phys. **106**, 7170 (1997).
[11] S. Lioyd, Science **273**, 1073 (1996).
[12] D. S. Abrams and S. Lioyd, Phys. Rev. Lett. **83**, 5162 (1999).
[13] E. Farhi, J. Golstone, S. Gutmann, J. lapan, A. Lundgren, and D. Preda, Science **292**, 472 (2001).
[14] R. Cleve, A. Ekert, C. Macchiavello, and M. Mosca, Proc. R. Soc. Lond. A **454**, 339 (1998).
[15] A. Aspuru-Guzik, A.D. Dutoi, P.J. Love, and M. Head-Gordon, Science **309**, 1704 (2005).
[16] H. Wang, S. Kais, A. Aspuru-Guzik, and M. R. Hofmann, Phys. Chem. Chem. Phys. **10**, 5388 (2008).
[17] R. Feynman, Int. J. Theor. Phys. **21**, 467 (1982).
[18] D. Deutsch, Proc. Roy. Soc. Lond. A **400**, 97 (1985).
[19] F. Bernstein and U. Vazirani, SIAM J. Comput. **26**, 1411 (1997).

[20] D. Simon, *Proceedings of 35th Annual Symposium on the Foundations of Computer Science* (IEEE Computer Society, Los Alamitos, 1994), p. 116, (Extended Abstract). Full version of this paper appears in SIAM J. Comput. **26**, 1474 (1997).
[21] L. Grover, *Proceedings of the 28th Annual ACM Symposium on the Theory of Computing* (ACM Press, New York, 1996), p. 212.
[22] P.W. Shor, presented at *Algorithms For Quantum Computation: Discrete Logs and Factoring*, Proceedings of the 35th Symposium on the Foundations of Computer Science **124** (1994).
[23] P.W. Shor, SIAM J. Comput. **5**, 1484 (1997).
[24] M. Garey and D. Johnson, *Computers and Intractability: a Guide to the Theory of NP Completeness* (W.H. Freeman and Co., San Francisco, 1979).
[25] C.H. Bennett, E. Bernstein, G. Brassard, and U. Vazirani, SIAM J. Comput. **26**, 1510 (1997).
[26] R. Jozsa, in *The Geometric Universe*, edited by S. Huggett, L. Mason, K.P. Tod, S.T. Tsou, and N. Woodhouse (Oxford University Press, Oxford, 1998), pp. 369–379.
[27] R. Jozsa, Proc. Roy. Soc. Lond. Ser. A **454**, 323 (1998).
[28] A. Ekert and R. Jozsa, Phil. Trans. Roy. Soc. Lond. Ser A **356**, 1769 (1998).
[29] F. Remacle and R.D. Levine, PNAS **101**, 12091 (2004).
[30] R. de Vivie-Riedle and U. Troppmann, Chem. Rev. **107**, 5082 (2007).
[31] L.K. Grover, Phys. Rev. Lett. **79**, 325 (1997).
[32] L.K. Grover, Phys. Rev. Lett. **95**, 150501 (2005).
[33] M.A. Nielsen and I.L. Chuang, *Quantum Computation and Quantum Information* (Cambridge University Press, Cambridge, 2000).
[34] M. Hirvensalo, *Quantumm Computing* (Springer-Verlag, Berlin, 2001).
[35] J.A. Jones, Science **280**, 229 (1998).
[36] M.O. Scully and M.S. Zubairy, PNAS **98**, 9490 (2001).
[37] A. Perdomo, C. Truncik, I.T. Brohman, G. Rose, and A. Aspuru-Guzik, Phys. Rev. A **78**, 012320 (2008).
[38] W.P. Baritompa, D.W. Bulger, and G.R. Wood, SIAM J. Optim. **15**, 1170 (2005).
[39] D.J. Wales and J.P.K. Doye, J. Phys. Chem. A **101**, 5111 (1997).
[40] R.S. Berry, T.L. Beck, H.L. Davis, and J. Jellinek, in *Advances in Chemical Physics*, edited by I. Prigogine and S.A. Rice (Wiley, New York, 1988), Vol. 70B, p. 75.
[41] L.T. Wille and J. Vennik, J. Phys. A **18**, L419 (1985).
[42] J.A. Northby, J. Chem. Phys. **87**, 6166 (1987).
[43] S.P. Jordan, Phys. Rev. Lett. **95**, 050501 (2005).
[44] L.M.K. Vandersypen, M. Steffen, G. Breyta, C.S. Yannoni, R. Cleve, and I.L. Chuang, Phys. Rev. Lett. **85**, 5452 (2000).
[45] E. Knill, R. Laflamme, R. Marinez, and C.H. Tseng, Nature (London) **404**, 368 (2000).
[46] R.J. Nelson, D.G. Cory, and S. Lloyd, Phys. Rev. A **2**, 2106 (2000).
[47] Z.L. Madi, R. Bruschweiler, and R.R. Ernst, J. Chem. Phys. **109**, 10603 (1999).
[48] R. Das and A. Kumar, J. Chem. Phys. **7601**, 121 (2004).
[49] Y.L. Ju, I.M. Tsai, and S.Y. Kuo, IEEE Trans. Circuits Systems I – Regular Papers **54**, 2552 (2007).
[50] N. Xu, J. Zhu, X. Peng, X. Zhou and J. Du, preprint arXiv:0809.0664v1 (2008).

Appendix

This Appendix shows how the modified Grover's algorithm is used for the simulation of the global minimum of the GP function. In the text, we used a total of 10 qubits for the optimisation. Here, as an example we provide results for only two qubits. One qubit is used to represent the x_1 axis and the other for the x_2 axis. The search range was $x_{1,2} \in [-3.2, 3.0]$ and discretised into $2^1 = 2$ points on each axis.

Step (1): Perform the Walsh–Hadamard transformation to place the system into a superposition with equal probabilities for all states. The obtained vector is also our original source $|s\rangle$. The formula for this step is $|s\rangle = \bigotimes_{i=1}^{2} H|0\rangle$. Thus, we obtain the vector $|s\rangle = (0.5\ .5,\ 0.5\ 0.5)^{\mathrm{T}}$.
Step (2): Generate the P_s operator, $P_s = 2|s\rangle\langle s| - I$, where $|s\rangle$ is the vector we obtain in Step 1. P_s increases the amplitude of the selected state and takes the form

$$P_s = \frac{1}{2}\begin{pmatrix} -1 & 1 & 1 & 1 \\ 1 & -1 & 1 & 1 \\ 1 & 1 & -1 & 1 \\ 1 & 1 & 1 & -1 \end{pmatrix}. \tag{7}$$

Step (3): Obtain the entry matching the search criterion $|t\rangle$ (can also be called the target source). There is no direct way to obtain the target source from the pure quantum method, so a 'black box' type is used in the current simulation. Thus, it was obtained by an indirect mapping. We calculated values of the GP function at all mesh points and picked the lowest one by classical comparison. Then we marked the corresponding part of $x_{1,2}$ as 1 and the rest as zeros. This was followed by applying the Kronecker tensor product to obtain the target source $|t\rangle$, which is a similar vector to $|s\rangle$. For this example, the point $(-3.2, -3.2)$ has the lowest value. The corresponding target source is $|t\rangle = (1\ 0)^{\mathrm{T}} \bigotimes (1\ 0)^{\mathrm{T}} = (1\ 0\ 0\ 0)^{\mathrm{T}}$.
Step (4): Generate the P_t operator, where $P_t = I - 2|t\rangle\langle t|$. This operator reverses the selected state and takes the form

$$P_t = \begin{pmatrix} -1 & 0 & 0 & 0 \\ 0 & 1 & 0 & 0 \\ 0 & 0 & 1 & 0 \\ 0 & 0 & 0 & 1 \end{pmatrix}. \tag{8}$$

Step (5): Apply the Grover operator, $G = P_s P_t$, $O(N^{1/2})$ times to the superposition state ($|s\rangle$). The new G operator has the effect of both P_s and P_t, which reverses the selected state first and then increases its amplitude. For this example, it takes the form

$$G|s\rangle = P_s P_t |s\rangle = P_s \begin{pmatrix} -0.5 \\ 0.5 \\ 0.5 \\ 0.5 \end{pmatrix} = \begin{pmatrix} 1 \\ 0 \\ 0 \\ 0 \end{pmatrix}. \tag{9}$$

For this simple example, we obtained the correct answer in one step.